

Primary-Fragment Angular Momenta in Deep-Inelastic Reactions

J. B. Natowitz, M. N. Namboodiri, P. Kasiraj, R. Eggers, L. Adler, P. Gonthier,
C. Cerruti, and T. Alleman

Cyclotron Institute and Department of Chemistry, Texas A & M University, College Station, Texas 77840
(Received 12 December 1977)

γ -ray multiplicities $\langle M_\gamma \rangle$ and energies $\langle E_\gamma \rangle$ associated with identified products of completely damped collisions of 237-MeV ^{40}Ar with ^{89}Y are analyzed to determine the angular momenta of the primary heavy fragments. Extending the analysis to the system 175-MeV $^{20}\text{Ne} + \text{Ag}$ allows a comparison which indicates that different partial waves contribute in these two nearly identical composite systems at almost the same excitation energy and that the transition from fusion-evaporation to deep-inelastic reactions occurs over a wide range of partial waves.

A determination of the angular momentum transfer in strongly damped collisions offers the possibility of exploring in detail the frictional forces acting between the two reaction partners. At least three recent experiments¹⁻³ suggest that a rigidly rotating dinuclear complex may be formed in the final stages of such collisions. γ -ray multiplicity measurements can be used to elucidate the question of angular momentum transfer is a reliable transition from the observed multiplicities to the primary-fragment angular momenta can be obtained. The extraction of the primary angular momentum is complicated by the fact that prompt continuum γ rays from both partners of the deep-inelastic reaction are detected. As the asymmetry of the mass split increases, the excitation energies and the angular momenta of the two fragments can be very different. As a result, approximations such as the assumption of 100% stretched quadrupole radiation are not generally sufficient to extract angular momenta with accuracy adequate to test various reaction models.

In this work we use measurements of the average total multiplicities $\langle M_\gamma \rangle$ and average energies $\langle E_\gamma \rangle$ to extract the average γ -ray multiplicities $\langle M_\gamma \rangle_H$ of the heavier partners of the deep-inelastic reactions in the system $^{40}\text{Ar} + ^{89}\text{Y}$ at 237 MeV. We then employ data on $\langle M_\gamma \rangle$ from fusion reactions to derive the angular momenta of the primary heavy fragments. The analysis is extended to the data² on the reactions of 175-MeV ^{20}Ne with Ag. A comparison of the two systems indicates that different partial waves lead to the detected product in each case. Further, the results indicate that competition between fusion-evaporation and deep-inelastic processes occurs over a wide range of partial waves.

Three 3-in. \times 3-in. NaI detectors placed at 35°, 90°, and 145° relative to the incident beam direction were employed to detect the γ rays in coin-

idence with reaction products detected in a detector telescope employing a gas ionization ΔE detector. Time-of-flight discrimination was used to separate the prompt γ radiations from neutrons. The methods of analyzing the pulse-height spectra to determine $\langle M_\gamma \rangle$ and $\langle E_\gamma \rangle$ are essentially those of Pleasonton *et al.*⁴ and Banaschik *et al.*⁵ and are reported in detail elsewhere.^{6,7}

Multiplicities and energies were determined from measurements taken with the detector telescope at 50° and 60° with respect to the incident beam direction, on the opposite side of the beam from the NaI detectors, in the same plane as the NaI detectors. One measurement was made with the telescope at 50° in a plane perpendicular to the plane of the NaI detectors. This latter measurement showed a decrease of approximately 30% in the coincidence rate of the 90° NaI detector. If alignment of the product angular momenta perpendicular to the reaction plane were complete and the γ -ray cascades were stretched this measurement suggests approximately equal mixtures of dipole and quadrupole radiations.

The average multiplicities $\langle M_\gamma \rangle$ and average energies $\langle E_\gamma \rangle$ are presented in Fig. 1 as a function of the atomic number of the identified reaction product. Also presented for comparison are data for the multiplicities reported for the reactions of 175-MeV ^{20}Ne with Ag, in which essentially the same composite system is produced with almost the same excitation energy. Thus the differences in the observed multiplicities already indicate differences in the angular momenta of the reaction products.

A conversion of multiplicities to average angular momenta is possible in principle if there are sufficient calibration data available. Such data would be the variation of $\langle M_\gamma \rangle$ with product mass, average angular momentum, and excitation energy. In Fig. 2(a), a contour diagram is presented in which recent measurements of $\langle M_\gamma \rangle$ are pre-

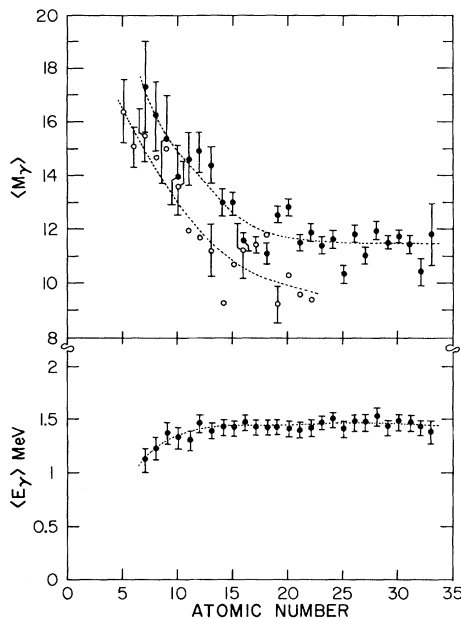


FIG. 1. Average multiplicities $\langle M_\gamma \rangle$ and average energies $\langle E_\gamma \rangle$ of products of completely damped reactions of 237-MeV ^{40}Ar with ^{89}Y (solid circles) and $\langle M_\gamma \rangle$ from Ref. 2 for 175-MeV ^{20}Ne with Ag (open circles).

sented as a function of the mass and the average angular momentum of the de-exciting nucleus.⁶⁻¹¹ The values of $\langle J \rangle$ are determined either from cross-section data or from a Bass-model calculation¹² of the limiting angular momentum for fusion.

It is clear from this figure that the γ -ray multiplicities are relatively sensitive to angular momentum for masses ≥ 70 amu and relatively insensitive to angular momentum at lower masses. Presumably this insensitivity at lower masses reflects the importance of the particle emission cascade as a means of angular momentum dissipation.⁶

The excitation energies of the compound nuclei for which data are presented in Fig. 2(a) vary considerably. Since the multiplicity for a particular $\langle J \rangle$ will also depend somewhat on the excitation energy, it would clearly be advantageous to have additional data to construct a more refined $\langle M_\gamma \rangle$ versus $\langle J \rangle$ calibration plot. However, in view of the fact that thermal equilibrium appears to be a very good assumption in completely damped collisions,^{13,14} the excitation energies of the heavier reaction products studied here should in fact be quite comparable to those for which the multiplicity data presented in Fig. 2(a) were taken. We emphasize that even though the angular

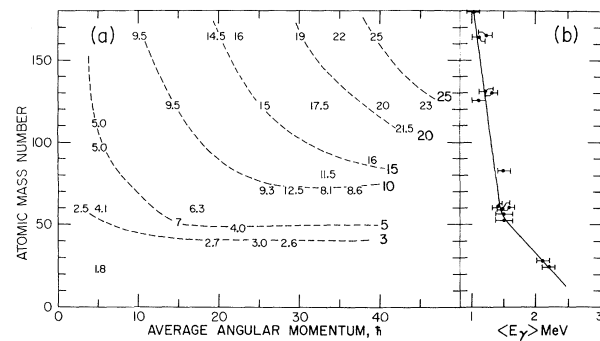


FIG. 2. (a) Contours of constant $\langle M_\gamma \rangle$ from the de-excitation of fusion products, in the A - $\langle J \rangle$ plane, with selected intermediate values. (Data from Refs. 6-11 and 15). (b) Recent data on $\langle E_\gamma \rangle$ from the de-excitation of fusion products; from Refs. 6-11 and 15.

momenta are to be determined from measurements of $\langle M_\gamma \rangle$, the effects of particle emission are also taken into account by the calibration technique.

Fortunately, the total multiplicities can, in fact, be separated into the multiplicities $\langle M_\gamma \rangle_H$ and $\langle M_\gamma \rangle_L$ associated with the heavy and light fragments, respectively. This is made possible by the fact that the average γ -ray energies of the products of interest in this investigation are a function of the mass number. This is illustrated in Fig. 2(b) where various data on the average energies $\langle E_\gamma \rangle$ for fusion reactions are presented as a function of the mass of the γ -decaying nucleus.^{6,7,11,15} We assume that these $\langle E_\gamma \rangle$ values are also applicable to the strongly damped fragments studied in the present work. If the angular momentum distributions of the fragments are very different from those of the fusion residues, the values of $\langle M_\gamma \rangle_H$ and $\langle M_\gamma \rangle_L$ derived below could be affected somewhat. Experimental clarification of this point would be very useful.

We assume that the mass of the detected fragment corresponds to the line of β stability and therefore that both masses may be determined from the measured atomic number with sufficient accuracy to determine the average energies $\langle E_\gamma \rangle_L$ from Fig. 2(b). We then use the relationships

$$\begin{aligned} \langle M_\gamma \rangle_H \langle E_\gamma \rangle_H + \langle M_\gamma \rangle_L \langle E_\gamma \rangle_L &= \langle M_\gamma \rangle \langle E_\gamma \rangle, \\ \langle M_\gamma \rangle_H + \langle M_\gamma \rangle_L &= \langle M_\gamma \rangle, \end{aligned} \quad (1)$$

to extract the multiplicities $\langle M_\gamma \rangle_H$ and $\langle M_\gamma \rangle_L$ from the smooth lines through the data of Fig. 1.

The results of this analysis are presented in Fig. 3 for the reactions of 237-MeV ^{40}Ar with ^{89}Y .

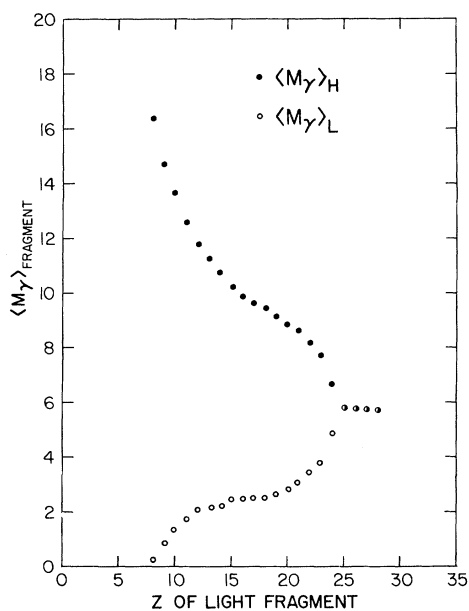


FIG. 3. Individual product γ -ray multiplicities $\langle M_\gamma \rangle_H$ and $\langle M_\gamma \rangle_L$, derived as described in the text, for 237-MeV $^{40}\text{Ar} + ^{89}\text{Y}$.

The solid circles in that figure represent the multiplicities $\langle M_\gamma \rangle_H$ of the heavier reaction partner. For large mass asymmetries, the major fraction of the γ rays clearly result from the heavier products. The lighter partners have low multiplicities, ~ 2 to 3 , over a wide mass range as is expected from the data in Fig. 2. As mass symmetry is approached, the sudden decrease in $\langle M_\gamma \rangle_H$ and the increase in $\langle M_\gamma \rangle_L$ occur near entrance into a mass region where the multiplicity becomes more sensitive to mass changes and less sensitive to angular momentum changes.

Combining the data for $\langle M_\gamma \rangle_H$ with the calibration data presented in Fig. 2 allows us to fix the angular momenta of the heavier primary fragments. The solid line in Fig. 4 represents the variation of the heavy-fragment angular momentum with fragment atomic number for the reactions of 237-MeV ^{40}Ar with ^{89}Y . Since the sensitivity of $\langle M_\gamma \rangle_H$ to angular momentum is less near symmetry, a better estimate of the angular momentum at symmetry may result from the short extrapolation of the smoothly varying angular momentum curve as is indicated.

In addition, the reaction of ^{20}Ne with Ag at 175 MeV leads to an almost identical composite system and excitation energy as the reaction of 237-MeV ^{40}Ar with ^{89}Y . Since the γ -ray multiplicity of the lighter fragment is very insensitive to angular momentum, the measured values of $\langle M_\gamma \rangle$

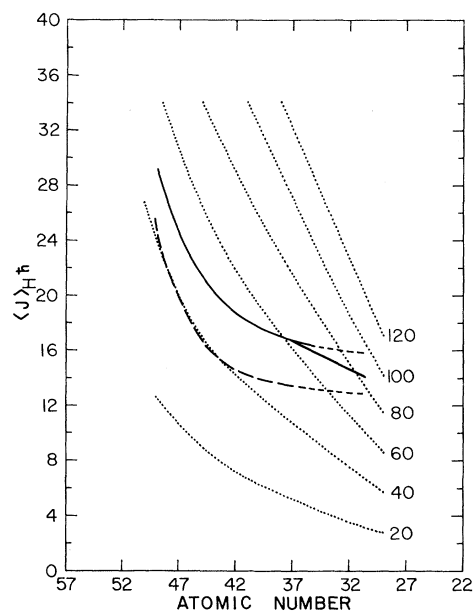


FIG. 4. The average angular momenta $\langle J \rangle_H$ of primary heavy fragments produced in deep inelastic reactions of 237-MeV ^{40}Ar with ^{89}Y (solid line) and of 175-MeV ^{20}Ne with Ag (dashed line). Both lines are extrapolated in the region of symmetry. The dotted line indicate the values of $\langle J \rangle_H$ which would result from particular initial values of l if the system may be represented as two touching, rigidly rotating spherical nuclei.

for the $^{20}\text{Ne} + \text{Ag}$ reaction may be corrected using the $\langle M_\gamma \rangle_L$ values from Fig. 3. As a result, $\langle J \rangle_H$ may also be determined for this reaction system. The dashed line in Fig. 4 shows the results of this analysis.

A comparison of the values of $\langle J \rangle_H$ in Fig. 4 with the heavy fragment multiplicities in Fig. 3 indicates that the ratio $\langle J \rangle_H / \langle M_\gamma \rangle_H$ (which includes angular momentum removed in the particle cascade) ranges from 1.8 to 2.8. This emphasizes the importance of having sufficient calibration data so that arbitrary assumptions about the multipolarity mixture of the γ cascade may be avoided. In contrast, the differences of 1.5 to 2.0 units in the values of $\langle M_\gamma \rangle_H$ for the two reaction systems translate to differences of (3 to 4) \hbar in $\langle J \rangle_H$ indicating that the *additional* γ rays emitted from the higher angular momentum fragments produced in the reactions $^{89}\text{Y}(^{40}\text{Ar}, X)$ are, in fact, quadrupole γ rays.

It is of interest to compare the angular momenta derived from the experimental data with those predicted by the assumption of a rigidly rotating dinuclear system consisting of two spheres in contact. The dotted lines in Fig. 4 show the an-

gular momenta to be expected for various incident partial waves leading to the dinuclear system. As has been suggested by Glässel *et al.*, the results suggest either that angular momentum transfer is not complete or that lower partial waves lead preferentially to the more asymmetric mass split.^{16,17} The present experiment cannot directly distinguish between these possibilities. However, in both reaction systems the data are taken at angles where damping of the initial kinetic energy is complete, indicating that in each case the rotating dinuclear system has achieved a dynamic equilibrium which would be expected to include the sharing of angular momentum.

While a more accurate shape parametrization might modify the calculated curves somewhat, the results suggest that partial waves of 50 to 90 lead to the observed products in the $^{40}\text{Ar} + ^{89}\text{Y}$ case while partial waves of 40 to 80 contribute in the $^{20}\text{Ne} + \text{Ag}$ system. Fission of compound nuclei may contribute to the observed variation with angular momentum.

For the reactions of ^{40}Ar with ^{89}Y at 237 MeV, the evaporation-residue sharp cutoff limit, based on interpolations of experimental cross sections,¹⁸ should be $\sim 73\hbar$. In the $^{20}\text{Ne} + \text{Ag}$ reaction at 175 MeV, the corresponding limit is $57\hbar$. Strongly damped collisions would be expected to be most likely above these limits. A comparison of the lower limits of the angular momenta leading to deep-inelastic reaction products with the sharp cutoff limits for evaporation residues indicates that there is a large region of overlap between

the partial waves leading to fusion evaporation and those leading to deep inelastic reactions.

This research was supported in part by the U. S. Department of Energy and the Robert A. Welch Foundation.

¹M. Ishihara *et al.*, The Institute of Physical and Chemical Research Cyclotron Report No. 35, 1975 (unpublished), and in Proceedings of the Symposium on Macroscopic Features of Heavy Ion Collisions, Argonne, Illinois, 1976, edited by D. G. Korar, ANL Report No. ANL/PHY 76-2 (to be published), Vol. II, p. 172.

²P. Glässel *et al.*, Phys. Rev. Lett. **38**, 331 (1977).

³D. Dyer *et al.*, Phys. Rev. Lett. **39**, 392 (1977).

⁴F. Pleasonton *et al.*, Phys. Rev. C **6**, 1023 (1972).

⁵M. V. Banaschik *et al.*, Phys. Rev. Lett. **34**, 892 (1975).

⁶K. A. Geoffroy *et al.*, to be published.

⁷K. A. Geoffroy *et al.*, to be published.

⁸J. H. Degnan *et al.*, Phys. Rev. C **6**, 2255 (1973).

⁹J. R. Beene *et al.*, to be published.

¹⁰J. O. Newton *et al.*, Phys. Rev. Lett. **38**, 810 (1977).

¹¹J. J. Simpson *et al.*, Nucl. Phys. **A287**, 362 (1977).

¹²R. Bass, Phys. Rev. Lett. **39**, 265 (1977).

¹³K. Van Bibber *et al.*, in Proceedings of the Symposium on Macroscopic Features of Heavy Ion Collisions, Argonne, Illinois, 1976, edited by D. G. Kovar, ANL Report No. ANL/PHY-76-2 (to be published), Vol. II, p. 811.

¹⁴B. Cauvin *et al.*, LBL Report No. LBL-5099 (unpublished).

¹⁵J. F. Mollenauer, Phys. Rev. **127**, 867 (1962).

¹⁶C. F. Tsang, Phys. Scr. **10**, 90 (1974).

¹⁷R. Babinet *et al.*, Nucl. Phys. **A258**, 172 (1976).

¹⁸H. Gauvin *et al.*, Phys. Lett. **58B**, 163 (1975).